AIP | Applied Physics Letters

Optical super-resolution by high-index liquid-immersed microspheres

Arash Darafsheh, Gary F. Walsh, Luca Dal Negro, and Vasily N. Astratov

Citation: Appl. Phys. Lett. **101**, 141128 (2012); doi: 10.1063/1.4757600
View online: http://dx.doi.org/10.1063/1.4757600
View Table of Contents: http://apl.aip.org/resource/1/APPLAB/v101/i14
Published by the American Institute of Physics.

Report Documentation Page

Form Approved
OMB No. 0704-0188

1. REPORT DATE	2. REPORT TYPE	3. DATES COVERED
05 OCT 2012		**00-00-2012 to 00-00-2012**

4. TITLE AND SUBTITLE	5a. CONTRACT NUMBER
Optical super-resolution by high-index liquid-immersed microspheres	5b. GRANT NUMBER
	5c. PROGRAM ELEMENT NUMBER
6. AUTHOR(S)	5d. PROJECT NUMBER
	5e. TASK NUMBER
	5f. WORK UNIT NUMBER
7. PERFORMING ORGANIZATION NAME(S) AND ADDRESS(ES) **University of North Carolina at Charlotte,Department of Physics and Optical Science,Center for Optoelectronics and Optical Communications,Charlotte,NC,28223-0001**	8. PERFORMING ORGANIZATION REPORT NUMBER
9. SPONSORING/MONITORING AGENCY NAME(S) AND ADDRESS(ES)	10. SPONSOR/MONITOR'S ACRONYM(S)
	11. SPONSOR/MONITOR'S REPORT NUMBER(S)

12. DISTRIBUTION/AVAILABILITY STATEMENT
Approved for public release; distribution unlimited

13. SUPPLEMENTARY NOTES

14. ABSTRACT

15. SUBJECT TERMS

16. SECURITY CLASSIFICATION OF:			17. LIMITATION OF ABSTRACT	18. NUMBER OF PAGES	19a. NAME OF RESPONSIBLE PERSON
a. REPORT **unclassified**	b. ABSTRACT **unclassified**	c. THIS PAGE **unclassified**	**Same as Report (SAR)**	**5**	

Optical super-resolution by high-index liquid-immersed microspheres

Arash Darafsheh,[1,a)] Gary F. Walsh,[2,3] Luca Dal Negro,[2] and Vasily N. Astratov[1,b)]
[1]*Department of Physics and Optical Science, Center for Optoelectronics and Optical Communications, University of North Carolina at Charlotte, Charlotte, North Carolina 28223-0001, USA*
[2]*Department of Electrical and Computer Engineering & Photonic Center, Boston University, 8 Saint Mary's Street, Boston, Massachusetts 02215, USA*
[3]*U.S. Army NSRDEC, Nanomaterials Science Team, Kansas Street, Natick, Massachusetts 01760, USA*

(Received 24 June 2012; accepted 21 September 2012; published online 5 October 2012)

It is experimentally shown that barium titanate glass microspheres with diameters (D) in the range 2–220 μm and with high refractive index ($n \sim 1.9$–2.1) can be used for super-resolution imaging of liquid-immersed nanostructures. Using micron-scale microspheres, we demonstrate an ability to discern the shape of a pattern with a minimum feature size of $\sim\lambda/7$, where λ is the illumination wavelength. For spheres with $D > 50$ μm, the discernible feature sizes were found to increase to $\sim\lambda/4$. Detailed data on the resolution, magnification, and field-of-view are presented. This imaging technique can be used in biomedical microscopy, microfluidics, and nanophotonics applications. © *2012 American Institute of Physics*. [http://dx.doi.org/10.1063/1.4757600]

In recent years, research into properties of artificial materials and structures has allowed for a remarkable increase in the optical resolution of imaging systems well beyond the classical diffraction limit. The ideal imaging device should be able to capture the sub-diffraction limited details of an object and project it into the far field with some magnification. Super-resolution imaging devices have been realized using solid immersion lenses,[1] near-field probes,[2] fluorescent,[3] nonlinear, and negative index materials,[4] plasmon gratings,[5] and hyperbolic[6,7] metamaterials. It should be noted, however, that the applications of these structures and devices have been impeded to some extent by their sophisticated engineering designs and various technical limitations.

In this context, the near-field microscopy using nanolenses,[8] microdroplets,[9] and especially, microspheres[10,11] emerged as a surprisingly simple way of achieving optical super-resolution. It has been demonstrated[10] that silica spheres with refractive index (n) about 1.46 and with diameters (D) in the range 2–9 μm convert the high frequency spatial frequencies of the evanescent field into propagating modes that can be used for far field imaging of these sub-diffraction-limited features by looking "through the microsphere" into a virtual image produced by the microsphere below the surface of the structure.

More recently, it has been shown that the super-resolution capability of this technique can be reinforced by semi-immersing the corresponding low-index microspheres in a liquid droplet, producing a sharper contrast with a comparatively smaller magnification factor.[11] It should be noted that although the imaging in the presence of the liquid is useful for biomedical applications, using semi-immersed spheres is technically complicated due to dynamical droplet's evaporation process which leads to gradually varying resolution and magnification of the optical setup. It has been argued, however, that the super-resolution effect cannot be expected[11] when the microsphere is absolutely submerged by the liquid layer.

It has been suggested that, on a fundamental level, there is a connection between the super-resolution strength of micrometer-scale spheres and their ability to focus light down to sub-diffraction-limited dimensions.[10] Such tightly focused beams termed "photonic nanojets"[12,13] and corresponding "nanojet-induced modes"[14,15] have been observed in single spheres and chains of spheres, respectively.[16,17] The calculations predicted maximal super-resolution strength for $n = 1.8$. It has been argued that for $n > 1.8$ the super-resolution strength should be reduced along with a range of micrometer-scale sphere diameters where this effect can be expected.[10]

In this work, we experimentally demonstrate that the super-resolution imaging by microspheres totally immersed in the liquid is possible if the index of spheres is higher than 1.9. Recently, barium titanate glass (BTG) microspheres with $n \sim 1.9$–2.1 have been optically characterized in an aqueous environment.[18,19] Here, by using micron-scale BTG microspheres immersed in isopropyl alcohol (IPA) with index 1.37, we demonstrate the ability to discern the features as small as $\sim\lambda/7$, where $\lambda = 550$ nm is the peak illumination wavelength. A schematic of the setup and a virtual image formation are illustrated in Figs. 1(a) and 1(b), respectively. For spheres with $50 < D < 200$ μm, the discernible feature sizes were found to increase to $\sim\lambda/4$. The super-resolution field-of-view (FOV) was found to linearly increase with D reaching extraordinarily large values (~ 30 μm) for ~ 200 μm spheres. The magnification of the virtual images was found to be within 2.5–4.5 range for spheres with D in 2–220 μm range.

Two types of samples containing point and line objects, as illustrated in Figs. 1(c) and 1(f), respectively, were studied. The samples with point objects, Fig. 1(c), were represented by 2D arrays of gold nanoparticle dimers (NPDs) with periods of 320 nm and 800 nm in x and y directions, respectively. Each dimer consisted of two gold nanocylinders with 120 nm diameters and 30 nm height (2 nm Cr and

a)Electronic mail: adarafs1@uncc.edu.
b)Electronic mail: astratov@uncc.edu.

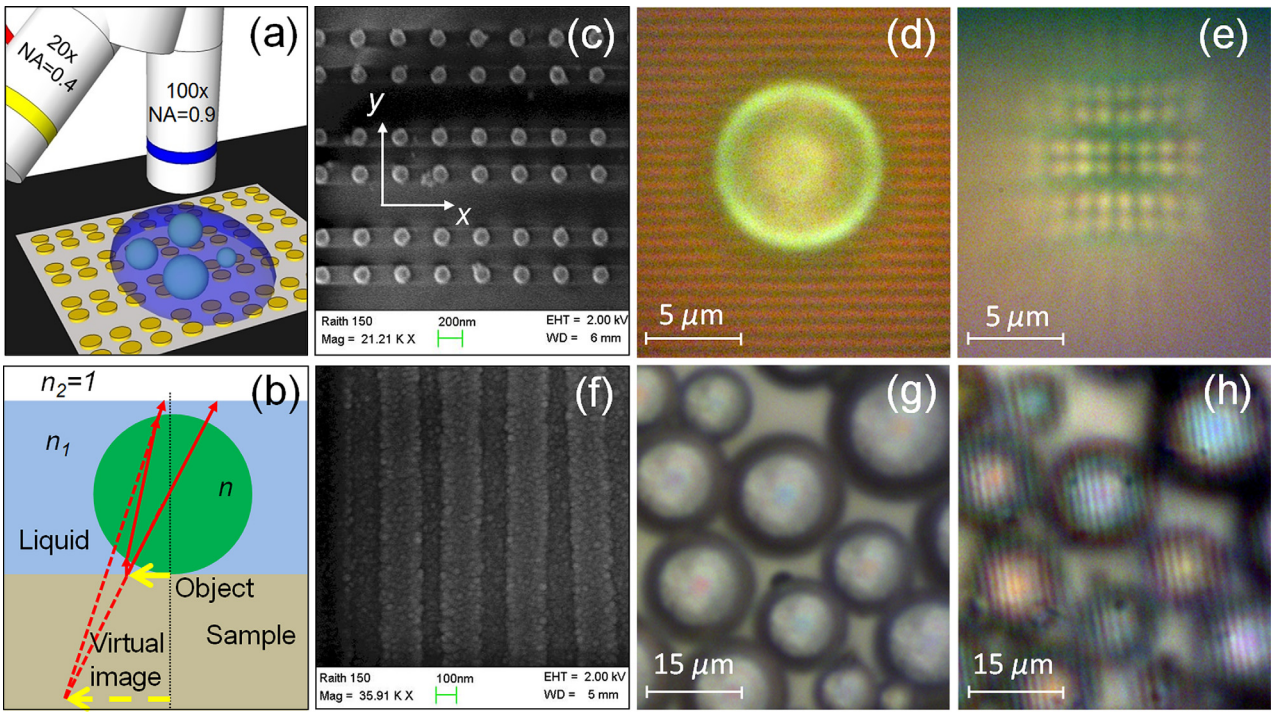

FIG. 1. (a) Schematic of the setup; (b) virtual image formation by a liquid-immersed sphere; (c) SEM image of an array of gold dimers formed by 120 nm nanoparticles with 150 nm separations; (d) BTG sphere with $n \sim 1.9$ immersed in IPA; (e) virtual imaging of the array shown in (c) through the microsphere at a different depth compared to (d) by 100× (NA = 0.9) objective; (f) SEM image of a Blu-ray disk with 200 nm width stripes separated by 100 nm width grooves; (g) BTG microspheres with diameters in the range ~5–20 μm fully immersed in IPA; and (h) virtual imaging of the Blu-ray disk through the microspheres at a different depth compared to (g) by 20× (NA = 0.4) objective.

28 nm Au) which were fabricated on a fused silica substrate by an electron beam lithography, metal evaporation, and lift-off process. The minimum edge-to-edge separations in dimers were 120 and 150 nm in different arrays. The SEM image in Fig. 1(c) represents NPDs with 150 nm separation (along y direction). The samples with linear objects were obtained using a commercial Blu-ray® disk (BD) with nominal track pitch sizes of 300 nm consisting of 200 nm width stripes separated by 100 nm width grooves as shown in Fig. 1(f). The 100-μm-thick transparent protection layer of the disk was peeled off before placing the microsphere. The NPDs sample was fabricated at BU, while the development of the imaging techniques was carried out at UNCC.

Two modifications of BTG microspheres (Mo-Sci Corp.) differing by their chemical composition and, as a result, by their index of refraction ($n \sim 1.9$ and ~2.1) were used. The microspheres were positioned on the samples using either micromanipulation or self-assembly. IPA was poured on the surface of the sample by a micro-syringe to totally cover the microspheres. Similar results were obtained using water infiltration.

An FS70 Mitutoyo microscope equipped with a halogen lamp and a CCD camera was used in reflection illumination mode with 100× (NA = 0.9) or 20× (NA = 0.4) microscope objectives. The system spectral response was strongly peaked at 550 nm. Using additional filters, we checked that all results are reproducible with narrow band (~20 nm bandwidth) illumination centered at 550 nm. Conventional microscopy allows resolving only the largest 800 nm period of the NPD array (along y direction) which is illustrated in Fig. 1(d) due to the stripe pattern outside the microsphere. Neither the 320 nm period, nor the 150 nm edge-to-edge separations in NPDs are resolved in this image. The 100 nm features in the BD also cannot be resolved.

We observed that the super-resolution imaging of the BD without liquid can be achieved using microspheres with small-to-moderate index of refraction such as borosilicate glass ($n \sim 1.47$), soda lime glass (~1.51), polystyrene (~1.59), and sapphire (~1.77). However, all these microspheres were found to completely lose their imaging capability, if they are completely covered with a liquid such as IPA.

High index ($n \sim 1.9$-2.1) BTG spheres showed a different behavior in these experiments. Without liquid addition, they did not produce any imaging. However, they provided super-resolution imaging in cases when they were totally covered with a liquid, as illustrated for point and linear objects in Figs. 1(e) and 1(h), respectively. The depth of focusing in these images is below the surface of the structure, as can be seen by comparison with conventional images of the same structures in Figs. 1(d) and 1(g), respectively. It is seen that the far field virtual images of individual gold nanoparticles with 120 nm diameters and 150 nm separations are resolved in Fig. 1(e). Similar resolution can be seen for a BD, as illustrated in Fig. 1(h). These results show an ability to discern the shape of a pattern with minimum feature size $\sim\lambda/4$, however, direct application of the Rayleigh criterion is complicated due to finite object sizes.

An important property for imaging applications is connected with the FOV which in previous studies was limited to a few microns due to the small diameters of low-index spheres.[8,10,11] We found that high-index liquid-immersed spheres preserve their super-resolution capability at significantly larger diameters. As shown in Figs. 2(a) and 2(b) for a sphere with $n \sim 1.9$ and $D \sim 125$ μm, the 150 nm separations

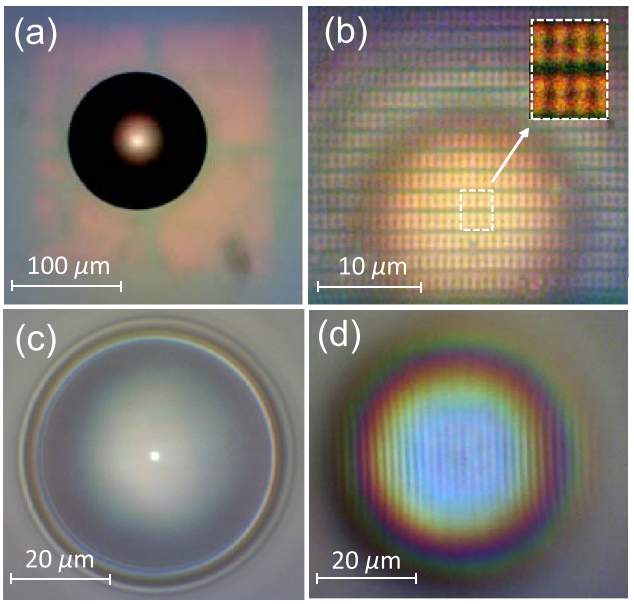

FIG. 2. (a) A BTG microsphere with $n \sim 1.9$ and $D \sim 125\,\mu$m fully immersed in IPA at the top of the NPD array with 150 nm separations, and (b) imaging through this microsphere by 100× (NA = 0.9) objective lens illustrating >20 μm super-resolution FOV; (c) BTG microsphere with $n \sim 2.1$ and $D \sim 53\,\mu$m fully immersed in IPA at the top of a BD, and (d) imaging through this microsphere by 20× (NA = 0.4) objective lens illustrating the 100 nm grooves of the BD.

in a NPD array are resolved by this sphere over an extraordinary large (~22 μm) FOV. Similar results were obtained for the BD sample using a sphere with $n \sim 2.1$ and $D \sim 53\,\mu$m totally immersed in IPA, as illustrated in Figs. 2(c) and 2(d).

The super-resolution strength of liquid-immersed high-index spheres stems from two factors. First, for sufficiently large spheres with size parameter $q = \pi D/\lambda \gg 100$, the resolution is improved by the reduction of λ in a liquid in a similar manner as it occurs in liquid-immersion type lens systems.[20] Second, for smaller values of the size parameter ($q < 100$), the super-resolution strength can be additionally enhanced[10] due to "photonic nanojet" properties of meso-scale spheres. The evanescent field plays a significant role in the field distribution close to the surface of the sphere for sufficiently large index contrasts;[21] however, the role of near-field evanescent waves in the super-resolution imaging mechanisms requires further study.

To study the dependence of the resolution capability on D, we used a NPD array with a 120 nm minimal separation illustrated in Fig. 3(a). The resolution was found to generally decrease with D, as illustrated in Figs. 3(b)–3(d). The intensity profiles were measured along the axis connecting two nanoparticles with a 120 nm separation, as illustrated in the insets to Figs. 3(b)–3(d). They display double peak structures which were fitted using two Gaussian peaks. The sums of Gaussian peaks are represented by dashed (red) curves in Figs. 3(b)–3(d). For 4.2 μm sphere, the minimal discernible feature sizes ~75 nm (~λ/7) can be estimated by assuming that two equally intense points are resolved when the intensity between them is 0.81. For $D = 53\,\mu$m spheres, the same criterion leads to the minimal discernible feature sizes ~λ/4.5.

The polarization effects were studied in the images of the BD samples by inserting a linear polarizer before the

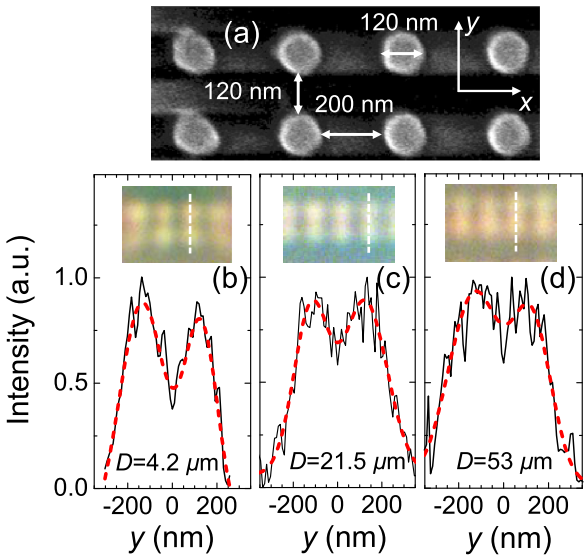

FIG. 3. (a) SEM image of an array of gold NPDs formed by 120 nm nanoparticles with 120 nm separations and resolving power of BTG microspheres with $n \sim 1.9$ and different diameters D: (b) −4.2 μm, (c) −21.5 μm, and (c) −53 μm. Insets show the optical microscope images obtained in (b)–(d) cases corresponding to SEM image in (a).

camera. If the polarizer axis is parallel to the BD stripes, the image has the minimal contrast, as illustrated in Fig. 4(a). The maximal contrast of the image was achieved with a polarizer axis perpendicular to the BD stripes, as shown in Fig. 4(c).

To study image magnification (M), we used microspheres with $n \sim 1.9$ and $2 < D < 220\,\mu$m, as illustrated in Fig. 5(a). The refraction law is determined by the index contrast, $n' = n/n_1 \sim 1.39$. For an object located at the sphere surface, the virtual image magnification can be estimated as $|M| \sim |n'/(2-n')| \sim 2.3$. For spheres with $D \sim 220\,\mu$m, where geometrical optics is expected to be a reasonable approximation, we measured $M \sim 2.5$. For the smallest spheres, $2 < D < 6\,\mu$m, where the geometrical ray tracing is not applicable, we observed increasing M with the spheres diameter similar to previous studies of imaging by low-index spheres in air.[10] In the intermediate diameter range, $6 < D < 10\,\mu$m, we found that M reaches the maximal values with significant variations from sphere to sphere in the 3.5–4.5 range, as illustrated in Fig. 5(a). It should be noted that the measurements of M were complicated by difficulties in reproducing the same depth of focusing on the virtual image. In addition, the image magnification increases with the distance from the optical axis due to the pincushion distortion which can be seen in Fig. 1(e) and in

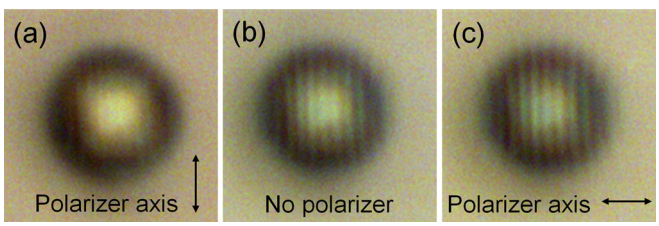

FIG. 4. BD samples imaged by a BTG microsphere with $n \sim 1.9$ with polarizer's axis (a) parallel to the stripes, (b) no polarizer, and (c) perpendicular to the stripes.

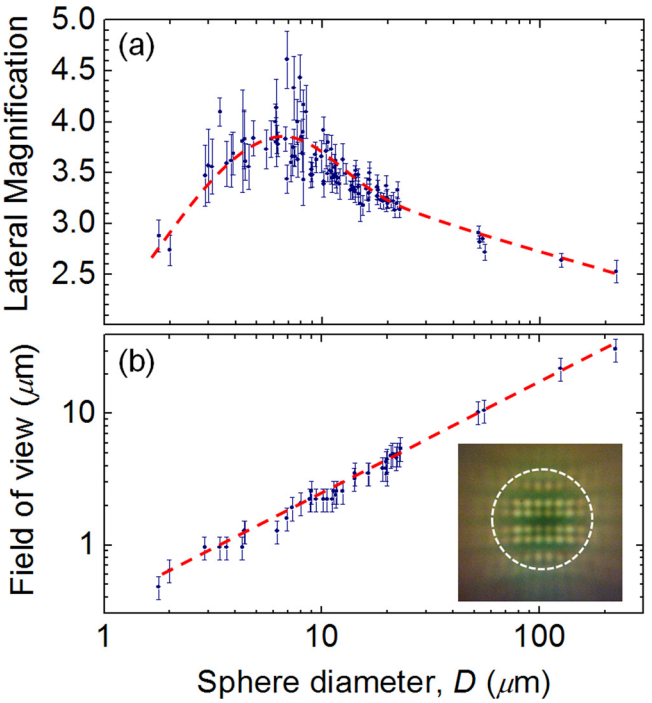

FIG. 5. (a) Lateral magnification and (b) FOV obtained by BTG microspheres with $n \sim 1.9$ as a function of D. The inset in (b) illustrates FOV for a sphere with $D = 9\,\mu$m. The measurements were performed using the NPD array. The dashed lines are guides for an eye.

the inset of Fig. 5(b) due to the fact that the lines formed by nanoparticles that do not go through the center of the image are bowed inwards, towards the center of the image. To diminish the role of the pincushion effect, we determined M in the central section of images. As illustrated in the inset to Fig. 5(b), FOV was defined as a diameter of the circle at the sample surface where we were able to discern the shape of the NPD array with the 150 nm separations. A close to linear dependence of FOV on D was observed, as shown in Fig. 5(b).

Projection imaging by microspheres has emerged as a surprisingly simple way of achieving far field super-resolution.[10,11] Many relevant optical properties of microspheres such as photonic nanojets,[12,13] nanojet induced modes,[14,15] and periodically focused modes[22] have been observed, stimulating applications of these structures in light focusing devices.[16,17,23] Applications of microspheres in biomedical microscopy often require liquid immersion of the samples which greatly reduces the index contrast of the imaging systems and diminishes their super-resolution capability. In this work, we solved this problem by using high index spheres in a liquid environment. For BTG microspheres ($n \sim 1.9$–2.1) with diameters on the order of several microns, we demonstrated the ability to discern the shape of a pattern with the minimum feature sizes $\sim\lambda/7$. For larger microspheres with $50 < D < 220\,\mu$m, the discernible feature sizes were found to increase to $\sim\lambda/4$. We observed that the super-resolution FOV linearly increases with D reaching extraordinary large values ($>30\,\mu$m) for $D > 200\,\mu$m. This property reduces the requirements to precise positioning of microspheres. These methods can be realized using spheres made from various high index materials such as titania or semiconductors. Depending on application, the structures can be infiltrated with water or with polymer materials. Due to its simplicity, the super-resolution imaging by high index microspheres can find many applications in biomedical microscopy, microfluidic devices, and nanophotonics.

The authors thank M. A. Fiddy, I. Vitebskiy, V. Kovanis, and D. M. Whittaker for stimulating discussions, A. D. Davies for sharing high NA microscope objective, and MO-SCI Corporation for donating some of the microspheres used in this work. This research was supported by the U.S. Army Research Office (ARO) through Dr. J. T. Prater under Contract No. W911NF-09-1-0450 and the National Science Foundation (NSF) under Grant No. ECCS-0824067. The fabrication work was supported by the U.S. Army Natick Soldier Center under Contract No. W911NF-07-D-001 and the SMART Scholarship Program, and has been approved for public release NSRDEC PAO#U12-307.

[1]B. D. Terris, H. J. Manin, D. Ruger, W. R. Studenmund, and G. S. Kino, Appl. Phys. Lett. **65**, 388 (1994).
[2]B. Hecht, B. Sick, U. P. Wild, V. Deckert, R. Zenobi, O. J. F. Martin, and D. W. Pohl, J. Chem. Phys. **112**, 7761 (2000).
[3]S. W. Hell, Science **316**, 1153 (2007).
[4]J. B. Pendry, Phys. Rev. Lett. **85**, 3966 (2000).
[5]I. I. Smolyaninov, Y. J. Hung, and C. C. Davis, Science **315**, 1699 (2007).
[6]Z. Jacob, L. V. Alekseyev, and E. Narimanov, Opt. Express **14**, 8247 (2006).
[7]Z. Liu, H. Lee, Y. Xiong, C. Sun, and X. Zhang, Science **315**, 1686 (2007).
[8]J. Y. Lee, B. H. Hong, W. Y. Kim, S. K. Min, Y. Kim, M. V. Jouravlev, R. Bose, K. S. Kim, I.-C. Hwang, L. J. Kaufman, C. W. Wong, P. Kim, and K. S. Kim, Nature **460**, 498 (2009).
[9]V. N. Smolyaninova, I. I. Smolyaninov, A. V. Kildishev, and V. M. Shalaev, Opt. Lett. **35**, 3396 (2010).
[10]Z. Wang, W. Guo, L. Li, B. Luk'yanchuk, A. Khan, Z. Liu, Z. Chen, and M. Hong, Nat. Commun. **2**, 218 (2011).
[11]X. Hao, C. Kuang, X. Liu, H. Zhang, and Y. Li, Appl. Phys. Lett. **99**, 203102 (2011).
[12]Z. G. Chen, A. Taflove, and V. Backman, Opt. Express **12**, 1214 (2004); S. Yang, A. Taflove, and V. Backman, *ibid.* **19**, 7084 (2011).
[13]P. Ferrand, J. Wenger, A. Devilez, M. Pianta, B. Stout, N. Bonod, E. Popov, and H. Rigneault, Opt. Express **16**, 6930 (2008); A. Devilez, N. Bonod, J. Wenger, D. Gérard, B. Stout, H. Rigneault, and E. Popov, *ibid.* **17**, 2089 (2009).
[14]A. M. Kapitonov and V. N. Astratov, Opt. Lett. **32**, 409 (2007).
[15]S. Yang and V. N. Astratov, Appl. Phys. Lett. **92**, 261111 (2008).
[16]For a review, see A. Heifetz, S. C. Kong, A. V. Sahakian, A. Taflove, and V. Backman, J. Comput. Theor. Nanosci. **6**, 1979 (2009).
[17]For a review, see V. N. Astratov, *Photonic Microresonator Research and Applications*, Springer Series in Optical Sciences Vol. 156, edited by I. Chremmos, O. Schwelb, and N. Uzunoglu (Springer, New York, 2010), pp. 423–457.
[18]A. Darafsheh, M. A. Fiddy, and V. N. Astratov, in *IEEE Proceedings of the 14th International Conference on Transparent Optical Networks–ICTON'12, Coventry, England, 2-5 July 2012* (IEEE, 2012), Paper No. Tu.A6.5, DOI: 10.1109/ICTON.2012.6254502.
[19]O. Svitelskiy, Y. Li, A. Darafsheh, M. Sumetsky, D. Carnegie, E. Rafailov, and V. N. Astratov, Opt. Lett. **36**, 2862 (2011).
[20]R. R. Kingslake, *Optical System Design* (Academic, London, 1983).
[21]A. Devilez, B. Stout, N. Bonod, and E. Popov, Opt. Express **16**, 14200 (2008).
[22]A. Darafsheh and V. N. Astratov, Appl. Phys. Lett. **100**, 061123 (2012).
[23]A. Darafsheh, A. Fardad, N. M. Fried, A. N. Antoszyk, H. S. Ying, and V. N. Astratov, Opt. Express **19**, 3440 (2011); T. C. Hutchens, A. Darafsheh, A. Fardad, A. N. Antoszyk, H. S. Ying, V. N. Astratov, and N. M. Fried, J. Biomed. Opt. **17**, 068004 (2012).